JOURNAL OF AIRCRAFT
Vol. 37, No. 4, July–August 2000

Comparison of Induced Velocity Models for Helicopter Flight Mechanics

R. E. Brown*
Imperial College of Science, Technology, and Medicine, London SW7 2BY, England, United Kingdom
and
S. S. Houston†
University of Glasgow, Glasgow G12 8QQ, Scotland, United Kingdom

Modeling of rotor-induced velocity receives continued attention in the literature as the rotorcraft community addresses limitations in the fidelity of simulations of helicopter stability, control, and handling qualities. A comparison is presented of results obtained using a rigid-blade rotor-fuselage model configured with two induced velocity models: a conventional, first-order, finite state, dynamic inflow model and a wake model that solves a vorticity-transport equation on a computational mesh enclosing the rotorcraft. Differences between the two models are quantified by comparing predictions of trimmed rotor blade flap, lag and feather angles, airframe pitch and roll attitudes, cross-coupling derivatives, response to control inputs, and airframe vibration. Results are presented in the context of measurements taken on a Puma aircraft in steady flight from hover to high speed. More accurate predictions of the cross-coupling derivatives, response to control, and airframe vibration obtained using the vorticity transport model suggest that incorporation of real flowfield effects is important to extending the bandwidth of applicability of helicopter simulation models. Unexpectedly small differences in some of the trim predictions obtained using the two wake models suggest that an overall improvement in simulation fidelity may not be achieved without equivalent attention to the rotor dynamic model.

Nomenclature

$\boldsymbol{a}$ = inflow state vector, m s^{-1}
a_x^{hinge}, a_z^{hinge} = hinge acceleration components, m s^{-2}
C_0 = apparent mass factor
$\boldsymbol{F}$ = aerodynamic forcing vector
I_{flap}, I_{lag}, I_{pitch} = blade moments of inertia, N m^2
$[\boldsymbol{L}]$ = inverse gain matrix
L_{aero} = aerodynamic rolling moment, N m
L_q = airframe roll acceleration due to pitch rate, s^{-1}
$L_{\theta_{1s}}$ = airframe roll acceleration due to longitudinal cyclic, s^{-2}
M_{aero} = aerodynamic pitching moment, N m
$M_{\text{flap}}^{\text{bl}}$, $M_{\text{lag}}^{\text{bl}}$ = blade flap and lag moments, N m
M_p = airframe pitch acceleration due to roll rate, s^{-1}
M_v = airframe pitch acceleration due to sideslip, m^{-1} s^{-1}
$M_{\theta_{1c}}$ = airframe pitch acceleration due to lateral cyclic, s^{-2}
n = number of blades
R = rotor radius, m
r = radial coordinate on rotor disk, m
S = vorticity source, s^{-2}
T_{aero} = aerodynamic thrust, N
t = time, s
$\boldsymbol{u}$ = control vector
v = flow velocity, m s^{-1}
v_m = wake mass-flow velocity, m s^{-1}
v_T = wake velocity, m s^{-1}
$\boldsymbol{x}$ = model state vector
$\boldsymbol{x}_{\text{rotor}}$ = rotor state vector
z = out-plane coordinate on rotor disk, m
α = local angle of attack, deg
β_0 = main rotor coning angle, deg
β_{1c} = main rotor longitudinal flapping, deg
β_{1s} = main rotor lateral flapping, deg
ζ_0 = main rotor mean lag angle, deg
ζ_{1s}, ζ_{1c} = first harmonic components of main rotor lag angle, deg
θ = fuselage pitch attitude, deg
θ_0 = main rotor collective pitch, deg
$\theta_{0_{\text{tr}}}$ = tail rotor collective pitch, deg
θ_{1c} = rotor lateral cyclic pitch, deg
θ_{1s} = rotor longitudinal cyclic pitch, deg
$[\boldsymbol{\tau}]$ = matrix of time constants, s
ϕ = fuselage roll attitude, deg
χ = wake skew angle, rad
Ψ = azimuthal coordinate on rotor disk, rad
ω = flow vorticity, s^{-1}
ω_x^{bl}, ω_y^{bl}, ω_z^{bl} = blade angular velocity components, rad s^{-1}

Introduction

THE mathematical modeling of stability, control, and handling qualities has assumed increased importance in the design and analysis of rotorcraft over the last 15 years. This has come about through a need to remedy known aircraft deficiencies and to provide real-time simulations of vehicle dynamics. Improvements in fidelity have come at the expense of complexity and computational effort, but increasing computer power continues to mitigate this.

Padfield's[1] threefold hierarchy of rotorcraft simulation models has proved useful for gauging the progress of the helicopter flight dynamics community toward a fully comprehensive analysis of the dynamic behavior of rotorcraft. In both level 1 and level 2 models, the velocity induced on the rotor disks is expressed as a superposition of a finite number of simple flow states in a first-order dynamic inflow model, but in a level 2 model the disklike representation of the rotors in a level 1 model is replaced by an individual-blade representation. In level 3 models the induced velocity near the rotors is calculated from an analysis of the detailed geometry of the entire rotor wake. Level 3 wake models have been in use in aerodynamic and structural-dynamic performance codes for some time, but implementation of wake models of this complexity in flight dynamics applications is uncommon.[2] Progress has been hindered largely by the

Received 23 August 1999; revision received 21 February 2000; accepted for publication 10 March 2000.

*Lecturer, Department of Aeronautics.
†Senior Lecturer, Department of Aerospace Engineering. Member AIAA.

computational intractibility imposed by the inherent disparity in the timescales associated with the rotor dynamics and aerodynamics and the timescale associated with the fuselage motions of the rotorcraft.

Finite state dynamic inflow models are preeminent in contemporary rotorcraft flight-dynamic simulations.[3,4] Their development is well summarized by Chen[5] and Gaonkar and Peters,[3] where the extensive literature attributed to Peters is rightly to the fore. Recent developments have tackled problems such as cross-coupling in a simple and elegant manner.[6,7] There is evidence, however, to suggest that some helicopter modeling deficiencies could result from unmodeled interactional effects in the rotor wake.[8,9] This paper is based on the premise that incorporation of these effects in a simulation model requires level 3 modeling of the rotor wake and presents calculations performed with a wake model, based on a numerical calculation of the transport of vorticity in the flow surrounding the rotorcraft, which is capable of embodying a variety of real flowfield effects such as wake distortion and main rotor/tail rotor and blade–vortex interactions. The objective of the paper is to quantify differences between the use of a simple dynamic inflow model, in which these effects are absent, and the new vorticity-transport wake model when each is coupled with a relatively standard, rigid individual-blade, rotor–fuselage helicopter dynamic model. This allows an assessment to be made of the impact of real flowfield effects on model fidelity.

In particular, predictions of rotor blade angle of attack vs azimuth for the two wake models are compared, and the presence of real flowfield effects in the predictions of the vorticity transport model are confirmed. Rotor blade flap, lag and feather angles, and airframe pitch and roll attitudes are compared for a helicopter in trimmed flight from hover to high speed. A limited comparison of the cross-coupling derivatives predicted using the two inflow models is then presented. Finally, we present comparisons, using the two inflow models, of the time response of the airframe to lateral cyclic control inputs and airframe vibration levels. The simulated data are presented in the context of results from flight experiments using a helicopter with conventional single main rotor/tail rotor configuration. This paper contributes to the literature in two ways: It presents a comprehensive flowfield formulation that is computationally attractive for flight mechanics applications, and it questions in a quantifiable manner the impact on helicopter flight mechanics simulations of some attributes of real wakes that hitherto have not been addressed.

Background

There is some evidence in the literature to suggest that real flowfield effects, such as wake distortion, main rotor/tail rotor wake interaction, and blade–vortex interaction, may have an impact on helicopter flight mechanics. Houston and Tarttelin[8] presented a comparison of heave dynamics in hovering flight predicted by a dynamic inflow disk-type model and identified from flight test. Although significant discrepancies could be removed by tuning the model with a series of physically justifiable correction factors, the near-uniform distribution of induced velocity predicted by the disk model bore little resemblance to the measured induced velocity field at the blade, which is momentumlike over a portion of the rotor disk but is significantly distorted by vortex interaction effects near the rotor tip and interference from the tail rotor. Padfield and Du Val[9] postulated that unmodeled tail rotor and main rotor wake interference may lead to similar discrepancies in forward flight.

The basic finite state formalism of Peters and co-workers has undergone continuous development to the point where dynamic inflow models are now almost exclusively used in the current generation of level 2 computational helicopter flight dynamics models.[10,11] Improved prediction of pitch–roll cross coupling has served as a particular focus for the development of the approach. Recently, extension of the model to mimic the effects of wake curvature,[6] and incorporation of delays on blade lift and drag,[7] has allowed a renewed attack on this problem. The Peters formalism is elegant, computationally highly efficient, and easy to incorporate into the state-space formalism of most coupled rotor–fuselage simulation models. These recent developments serve to retain the approach as an ideal tool for investigation of a range of helicopter flight mechanics problems, and the dynamic inflow approach is the benchmark with which all other approaches should be compared.

In general, the dynamic inflow formalism relies on a modal expansion of the velocity surrounding the rotorcraft as

$$v(r, \Psi, z) = \boldsymbol{a}(t) \cdot \boldsymbol{V}(r, \Psi, z) \tag{1}$$

where $\boldsymbol{V}(r, \Psi, z)$ is a finite dimensional vector of velocity distributions. The evolution of the vector of inflow states $\boldsymbol{a}(t)$ is usually governed by a nonlinear first-order equation of the form

$$[\boldsymbol{\tau}(\boldsymbol{a}, \dot{\boldsymbol{x}}_{\text{rotor}})]\dot{\boldsymbol{a}} + \boldsymbol{a} = [\boldsymbol{L}(\boldsymbol{a}, \dot{\boldsymbol{x}}_{\text{rotor}})]\boldsymbol{F} \tag{2}$$

where wake distortions are taken into account through the dependence of $[\boldsymbol{\tau}]$ and $[\boldsymbol{L}]$ on the rates of change $\dot{\boldsymbol{x}}_{\text{rotor}}$ of the states defining the rotor orientation.[6]

Unfortunately, the dynamic inflow formalism becomes less computationally efficient[12] as the number of modes describing the inflow distribution near the rotor is increased, and, although the approach is formally applicable to arbitrary rotor loading conditions, the formalism does not retain sufficient off-rotor information to represent fully the physics of the flow in the wake. For instance, blade–vortex interactions and the effects of wake rollup are not captured by the approach.[12] Stated equivalently, the strong influence of autoconvection of vorticity[13] on the evolution of wake structure, especially in the presence of interactive flow effects, suggests that one or more of the off-rotor modes, the inclusion of which may be essential to the encapsulation of certain aspects of the interactional flows, may be controlled only weakly, or even not at all, by the aerodynamic loading on the rotors. These off-rotor modes will not appear naturally (through the inclusion of their inflow states) in a dynamical system of the form of Eq. (2). It is, thus, to be expected that a model that is capable of more faithfully and robustly representing the fluid dynamic processes occurring in the wake would be more appropriate to flight dynamic analyses in the presence of strong aerodynamic interactions.

Mathematical Model

Rotor–Fuselage Model

The current implementation of the coupled rotor–fuselage model used in this paper employs a blade-element formulation to calculate the aerodynamic loads on each individual blade of the helicopter. The model has been used previously for helicopter validation and simulation studies[14,15] and for the simulation of autogyros.[16] Further properties of the model are summarized in Table 1.

The individual blade motions are governed by the standard rigid-body dynamic equations[17]

$$\begin{aligned} I_{\text{flap}}\left(\dot{\omega}_x^{\text{bl}} + \omega_y^{\text{bl}}\omega_z^{\text{bl}}\right) - m^{\text{bl}} y_{\text{cg}}^{\text{bl}} a_z^{\text{hinge}} &= M_{\text{flap}}^{\text{bl}} \\ I_{\text{pitch}}\left(\dot{\omega}_y^{\text{bl}} + \omega_x^{\text{bl}}\omega_z^{\text{bl}}\right) &= M_{\text{pitch}}^{\text{bl}} \\ I_{\text{lag}}\left(\dot{\omega}_z^{\text{bl}} + \omega_x^{\text{bl}}\omega_y^{\text{bl}}\right) - m^{\text{bl}} y_{\text{cg}}^{\text{bl}} a_x^{\text{hinge}} &= M_{\text{lag}}^{\text{bl}} \end{aligned} \tag{3}$$

Table 1 Rotor–fuselage model

Properties	Characteristics
Rotor dynamics (each rotor)	Up to 10 individually modeled rigid blades Fully coupled flap, lag, and feather motion Blade attachment by offset hinges and springs Linear lag damper
Rotor loads	Aerodynamic and inertial loads represented by up to 20 elements per blade
Blade aerodynamics	Lookup tables for lift and drag as function of angle of attack and Mach number
Transmission	Coupled rotorspeed and engine dynamics Up to three engines Geared or independently controlled rotor torque
Airframe	Fuselage, tailplane, and fin aerodynamics by lookup tables or polynomial functions
Atmosphere	International Standard Atmosphere Provision for variation of sea-level temperature and pressure

where expressions for the blade angular velocities ω_x^{bl}, ω_y^{bl}, and ω_z^{bl} and the hinge acceleration terms a_x^{hinge} and a_z^{hinge} are derived using standard kinematic principles.[14] The applied moment terms $M_{\text{flap}}^{\text{bl}}$ and $M_{\text{lag}}^{\text{bl}}$ include spring restraint terms if appropriate, and the lag degree of freedom embodies a linear lag damper term. The aerodynamic and inertia loads are transferred to the airframe via appropriate transformation to airframe-fixed hub coordinates following summation over blade elements.[14] The equations of motion of the airframe are written in standard state-vector form

$$\dot{\boldsymbol{x}} = f(\boldsymbol{x}, \boldsymbol{u}) \tag{4}$$

where $\boldsymbol{x}$ contains the airframe translational and angular velocity, blade flap, lag and feather angles and rates for each blade on each rotor, the angular velocity of each rotor, and the engine torques. The control vector $\boldsymbol{u}$ is aircraft configuration-specific, but for conventional single main and tail rotor configurations there are three main rotor controls and one tail rotor control. Equation (4) is then integrated to obtain the unsteady motion of the rotorcraft. Trim in steady flight is achieved by successive approximation to a state in which the mean forces and moments on the airframe are zero over a period that is long compared to the main rotor's rotational period.[14]

The rotor–fuselage model is, thus, a very conventional individual-blade/blade-element representation of a generic two-rotor aircraft, described by its blade mass distribution, blade aerodynamic properties, rotor hinge offset and restraint, the location and orientation of the rotors on the airframe, and the airframe's mass distribution and rudimentary aerodynamic characteristics.

Wake Modeling

The rotor–fuselage model is structured to allow selection of either a dynamic inflow model or the vorticity-transport model, both described in this section, to predict the local velocity at each of the blade elements.

Dynamic Inflow Model

The simple three-state dynamic inflow representation employed in this work is taken from Chen,[5] although the original model development is due to Peters (see Refs. 3 and 4). Note that, in the present formulation, the dynamic inflow formalism described hereafter is applied independently to each rotor in turn, and, hence, rotor interaction cannot enter the simulation through aerodynamic coupling of the rotors.

When we adopt the form of Eq. (1), the vector of flow modes

$$\boldsymbol{V}(r, \Psi) = [1, r\sin\Psi, r\cos\Psi] \tag{5}$$

models the distribution of wake velocity normal to the plane of each rotor, whereas Eq. (2) is forced by the vector of rotor aerodynamic loads

$$\boldsymbol{F} = [T_{\text{aero}}, L_{\text{aero}}, M_{\text{aero}}]^T \tag{6}$$

The matrix of time constants

$$[\tau] = \begin{bmatrix} \dfrac{4R}{3\pi v_T C_0} & 0 & \dfrac{-R\tan(\chi/2)}{12 v_m} \\ 0 & \dfrac{64R}{45\pi v_m(1+\cos\chi)} & 0 \\ \dfrac{5R\tan(\chi/2)}{8 v_T} & 0 & \dfrac{64R\cos\chi}{45\pi v_m(1+\cos\chi)} \end{bmatrix} \tag{7}$$

whereas the inverse gain matrix

$$[\boldsymbol{L}] = \frac{1}{\rho\pi R^3}\begin{bmatrix} \dfrac{R}{2v_T} & 0 & \dfrac{15\pi\tan(\chi/2)}{64 v_m} \\ 0 & \dfrac{-4}{v_m(1+\cos\chi)} & 0 \\ \dfrac{15\pi\tan(\chi/2)}{64 v_T} & 0 & \dfrac{-4\cos\chi}{v_m(1+\cos\chi)} \end{bmatrix} \tag{8}$$

Vorticity Transport Model

In an incompressible flow the velocity v anywhere in the neighborhood of the rotorcraft is related by the Poisson equation

$$\nabla^2 v = -\nabla \times \omega \tag{9}$$

to the vorticity $\omega = \nabla \times v$ in the flow surrounding the rotorcraft. Under the further assumption of limitingly small viscosity, the Navier–Stokes equation for the flow reduces to the unsteady vorticity-transport equation

$$\frac{\partial}{\partial t}\omega + v\cdot\nabla\omega - \omega\cdot\nabla v = S \tag{10}$$

where the source S is a function of the aerodynamic loads on the airframe and rotors and is nonzero only where aerodynamic forces are being generated.

Recently, Brown[13] has developed a grid-based algorithm for the solution of Eqs. (9) and (10) in helicopter aeromechanical applications. The equations are solved numerically by tesellating the domain surrounding the rotorcraft into a large number of three-dimensional cells and approximating v and ω by vector fields that are cellwise constant. Equation (9) is then solved by cyclic reduction,[18] and Eq. (10) is marched through time using Toro's weighted average flux (WAF) algorithm.[19] A particular advantage of the WAF algorithm is that it allows the effects of numerical diffusion of vorticity, which have plagued the accuracy of many previous attempts to construct grid-based numerical solutions of Eq. (10), to be reduced to very small levels. An important feature of the present vorticity transport model is that Eq. (10) is solved only after we recast it into a form that specifically conserves vorticity in parts of the computational domain where the vorticity source is zero. The particular advantage of such a formulation in the context of helicopter flight mechanics is that there then exists a natural decomposition of the equations governing the fluid dynamics that can be exploited numerically to allow the computational time constraint imposed by the disparate rotor and body–wake timescales to be overcome.[13]

The vorticity transport model is coupled into the rotor–fuselage simulation by using the aerodynamic loads generated by the blade-element model to construct S in terms of the shed and trailed vorticity from the blades of the rotors. The velocity at each blade element of each rotor is obtained by our sampling the field v at the location of the quarter-chord of the blade element. Specific details of the numerical implementation of this wake model, and some examples verifying the predictions of the basic approach, are presented by Brown.[13]

With the vorticity transport approach, interactions between the wakes shed by multiple blades on multiple rotors are naturally accounted for by direct solution of the fluid dynamic equations governing the wake's evolution. In this way, the assumptions made by the dynamic inflow formalism as to the modal structure of the flow and the dynamic form of the wake's evolution are circumvented.

Results

Flight Experiments

The aircraft used for the flight experiments was the SA330 Puma helicopter, formerly operated by the Defence Evaluation and Research Agency (DERA) at Bedford, England, United Kingdom, shown in Fig. 1. This aircraft was fully instrumented with two

Fig. 1 DERA Research Puma XW241.

separate inertial systems for measuring translational accelerations, angular rates, and attitudes. A probe-mounted air data system measured airspeed, sideslip, and angle of attack. Pilot control positions were also recorded. The flap, lag, and feather angles of each blade were measured with potentiometers, and local blade angle of attack could be inferred from a suite of pressure sensors and strain gauges attached to one of the blades.[8] Steady flights were conducted between hover and 150 kn, at a nominal altitude of 3000 ft and at weights between 5100 and 5800 kg. The simulations were configured with the actual flight conditions and weights recorded at each test point.

Rotor Aerodynamic Environment

Figure 2 shows comparisons between the azimuthal variation of angle of attack calculated using the dynamic inflow model and the vorticity transport model, and the flight data extracted by Padfield[1] and Houston and Tarttelin.[8] Clearly visible in the forward flight experimental data is the ridge corresponding to interaction with the tip vortex trailed from the preceding blade, whereas a secondary interaction somewhat farther inboard is less easily discernible. These interactive features are well represented by the vorticity transport model, but are entirely absent from the simulation using the three-state dynamic inflow model. Similarly, at hover, the vorticity transport model again reproduces the experimentally observed distortion of the loading pattern from the simple momentumlike structure predicted by the dynamic inflow model. Near the rotor tip, the interaction with the tip vortices from preceding blades manifests itself as a ridge of high angle of attack, whereas the asymmetry between the angle of attack in the aft quadrants of the rotor is primarily a result of interaction with the tail rotor.

Trim Parameters

Figures 3 and 4 present comparisons between simulations incorporating the Peters dynamic inflow model and the vorticity transport model. The results presented here show an obvious deficiency in the modeling of the overall drag on the vehicle at high speed, which manifests itself as an underprediction of the required main rotor collective pitch and consistent behavior of the longitudinal cyclic pitch, longitudinal flapping, and tail rotor collective pitch at speeds above 100 kn. The presence of this systematic error in the model strictly limits direct comparison of flight data and model predictions to speeds between 30 and 100 kn. Nevertheless, the small observed

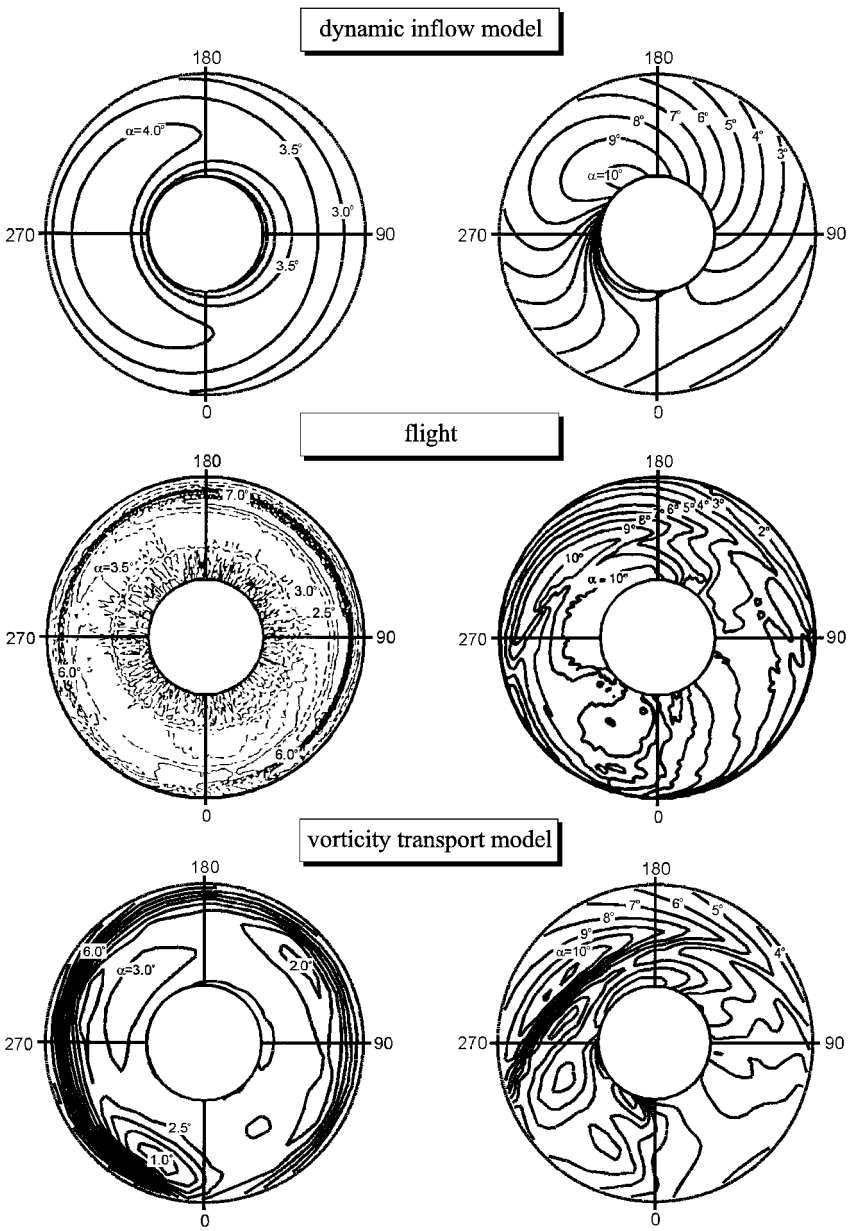

Hover **100kn**

Fig. 2 Rotor aerodynamic environment.

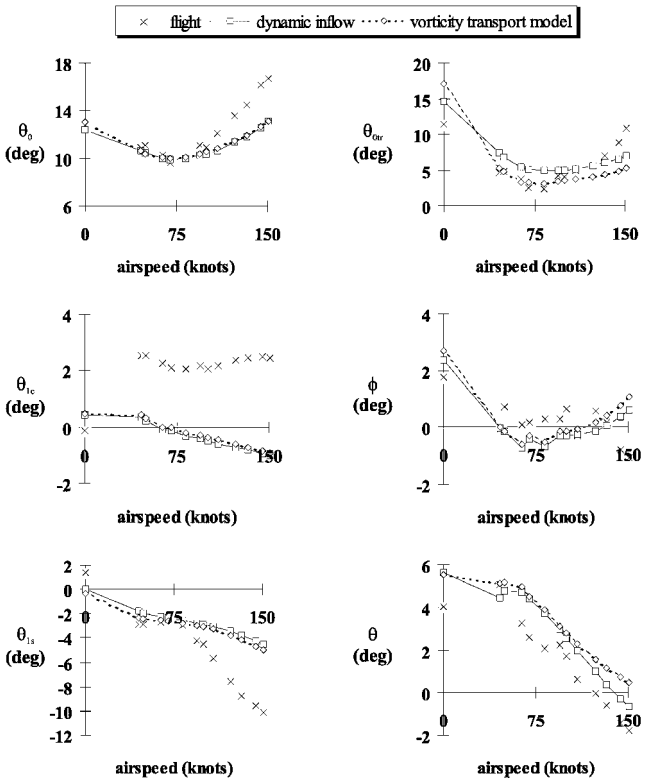

Fig. 3 Comparison of rotor control and aircraft angles.

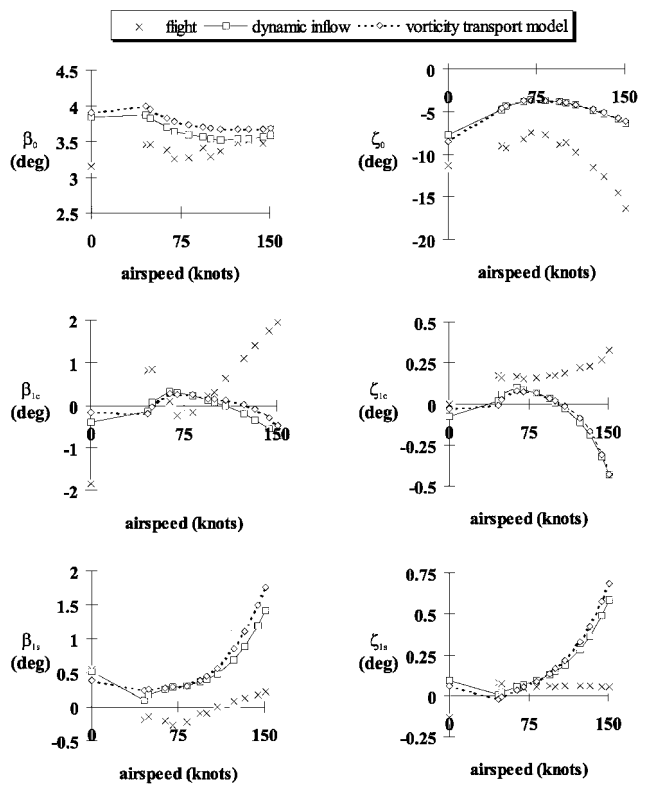

Fig. 4 Comparison of rotor flap and lag angles.

differences between the predictions of the longitudinal trim parameters using the two induced velocity models, and the good agreement with flight data in the range of validity of the airframe aerodynamic model, serve to validate the predictions of both induced velocity models. The interference between main and tail rotors (unmodeled, as described earlier, in our particular implementation of the dynamic inflow model) appears to be represented appropriately by the vorticity transport model because it accurately predicts tail rotor collective pitch up to 100 kn, whereas the dynamic inflow model

Table 2 Stability and control derivatives[a]

Derivative	Dynamic inflow	Vorticity transport	Flight identified[20]
M_v	0.004	−0.022	−0.021 (0.0015)
L_q	0.638	0.509	0.420 (0.0762)
M_p	−0.152	−0.103	−0.035 (0.0237)
$L_{\theta_{1s}}$	−2.904	−4.256	−2.822 (0.9620)
$M_{\theta_{1c}}$	2.327	4.512	—— (——)

[a]80 kn.

overestimates the tail rotor collective by around 2 deg (that is, by about 5% of control authority). The flight-measured lateral cyclic pitch and flapping are poorly predicted, but the similarity between the predictions by both inflow models of the lateral trim parameters throughout the speed range is most remarkable.

Low-Frequency Dynamics

Similar comparisons to the preceding are now presented for the low-frequency unsteady motion of the rotorcraft. Any model will be challenged by its ability to improve the prediction of pitch–roll cross coupling, an issue of great current interest to the helicopter flight dynamics community. Unfortunately, a comprehensive comparison of the classical six-degree-of-freedom stability and control derivatives for the Puma is presently compromised by an incomplete and inconclusive database for the full-scale aircraft.[20] In Table 2, preliminary predictions of some of the more important cross-coupling derivatives are compared against values identified at Glasgow University.[20] Standard deviations of the identified derivatives are given in parentheses. In all cases, significant separation between the predictions of the dynamic inflow model and the vorticity transport model is seen, and, arguably, the predictions of the vorticity transport model bear a closer relationship to the identified values, except in the case of the control derivative $L_{\theta_{1s}}$, where the large standard deviation suggests that the derivative was poorly identified from the flight data. Of particular note is the good agreement with the identified value of the vorticity transport model's prediction of M_v, a derivative estimated with high confidence from the flight data and of particular importance to the Puma's characteristic coupled pitch response in the Dutch roll mode.[20] The results presented here provide only a limited insight into the behavior of the two induced velocity models in predicting the low-frequency unsteady motion of the rotorcraft, and we hope to address the prediction of the classical stability and control derivatives more comprehensively in a later paper. Some further insight into the nature of the modeling differences can be obtained by comparing the response of each model to a lateral cyclic pitch control input, as shown in Figs. 5 and 6. Note that the responses are normalized by the peak roll rate in each case to clarify the relative differences between each model and flight test data. Although both models give a good account of the phasing and magnitude of the on- and off-axis responses, the simulation with the vorticity transport wake model exhibits features that render it superior for the prediction of the primary response to control input, as well as the cross-coupled response, at least in the short term. The divergence in pitch rate evident in the longer-term dynamics of both models appears to be due to an unstable phugoid-type oscillation that is not represented in the flight data.

Vibration

Finally, comparisons are extended to the high-frequency dynamics of the rotorcraft. Figure 7 shows time histories of the vertical acceleration of the center of gravity of the aircraft as measured in flight, together with results from simulation with both wake models. These results, for 90 kn, are typical of those found throughout the speed range. It is clear that the vorticity transport model gives a much better prediction of the amplitude of the 4 per revolution vibration than the dynamic inflow model. This is emphasized if the data in Fig. 7 are transformed into the frequency domain, as shown in Fig. 8. Neither model captures the 1 and 2 per revolution content of the vibration spectrum, but this discrepancy can be traced to a blade tracking error on the full-scale aircraft and, hence, is a feature unrelated to the modeling of the rotor wake.

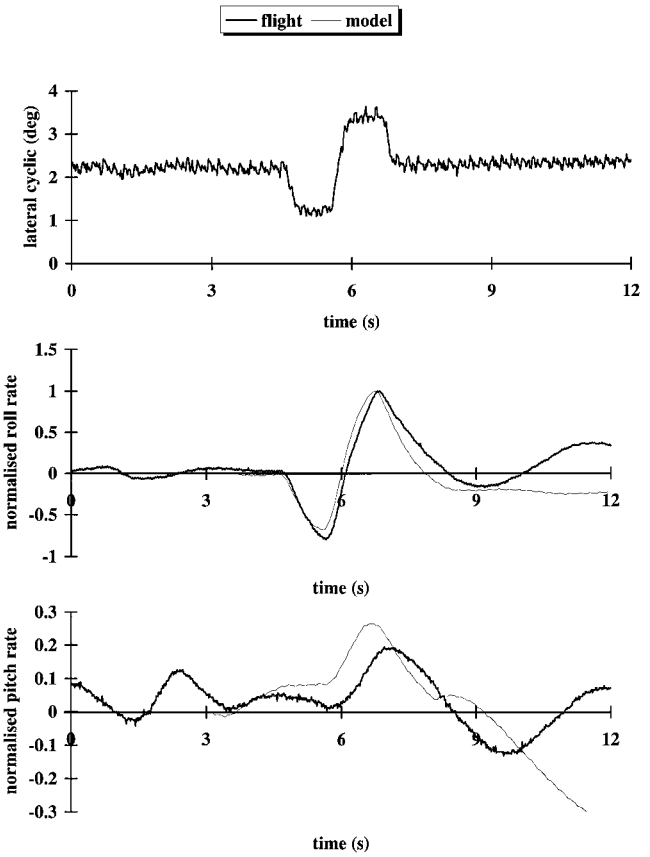

Fig. 5 Response to lateral cyclic at 80 kn, flight and dynamic inflow model.

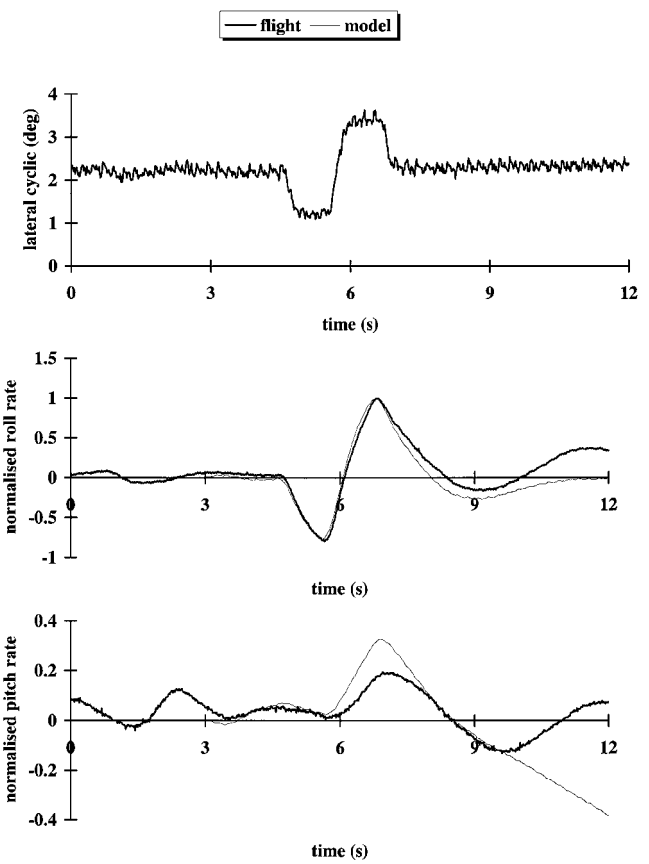

Fig. 6 Response to lateral cyclic at 80 kn, flight and vorticity transport model.

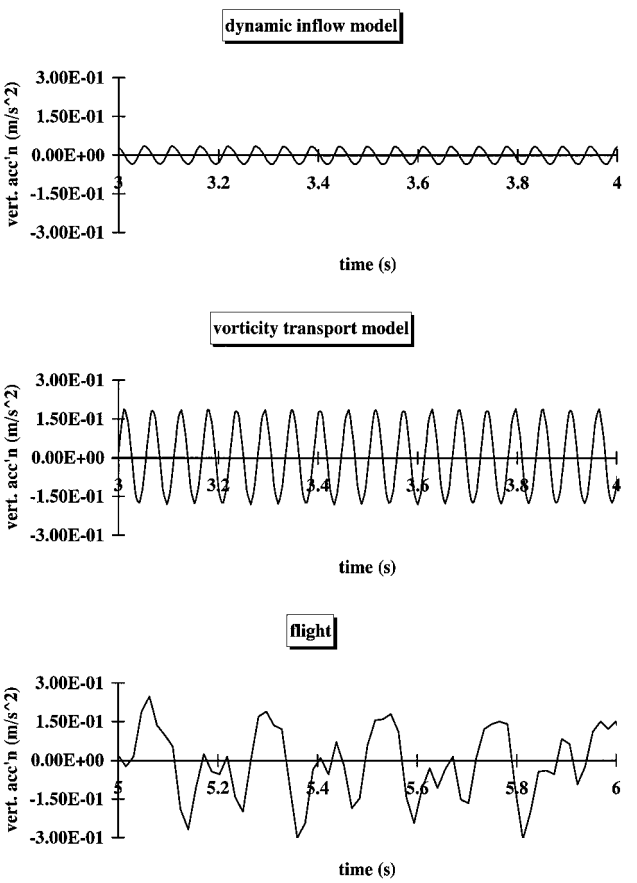

Fig. 7 Comparison of vertical acceleration, 90 kn.

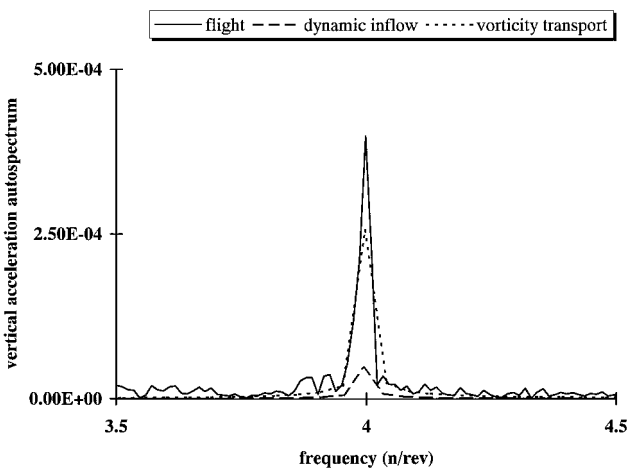

Fig. 8 Comparison of 4 per revolution component of vertical acceleration, 90 kn.

Discussion

The primary objective of this paper was to examine the significance of the incorporation of real flowfield effects, such as blade–vortex interaction and main rotor/tail rotor interaction, on the prediction of the flight mechanics of helicopters. Previous work had suggested that the omission of such effects by use of the dynamic inflow formalism to represent the rotor wake was largely responsible for the discrepancies between the predictions of typical coupled rotor–fuselage models and flight experiments.

Away from trim, it would indeed appear that the improved resolution of the real flowfield effects afforded by the vorticity transport model results in improved fidelity of simulation. Improved prediction of the cross-coupling derivatives, response to control input, and of the amplitude of the n per revolution vibration using the vorticity transport model suggests that incorporation of real flow

effects is an important contributory factor to the extension of the bandwidth over which flight dynamic models are valid and may indeed be necessary before integrated study of flight mechanics, vibration, and control become feasible. Yet, close analysis of the trim predictions obtained with the two inflow models confers somewhat more structure on this rather simplistic interpretation of the results presented so far.

In particular, the strong similarity between the main rotor lateral trim predictions obtained with the two induced velocity models, which persists even where agreement with flight data is poor, is somewhat surprising. Even more interesting is that close agreement is obtained despite the obviously disparate rotor-loading distributions predicted by the two models. The observed similarity is most likely a consequence of the rigid-blade dynamic model's transmission to the rotor shaft of only the zeroth- and first-order moments of the radial loading distribution on the blades. Because the trim procedure described earlier is sensitive only to the loads transmitted to the airframe through the rotor shaft, the rotor parameters predicted with the two inflow models will be driven in trim to states that are equivalent to first order in their resultant radial loading distribution on the blades. A qualitative illustration of the relative insensitivity of the trim procedure to the detailed structure of the loading distribution on the main rotor is obtained by contrasting the azimuthal distributions of angle of attack predicted with the two inflow models. The effects of the blade dynamic model are most clearly evident in the hover angle-of-attack distribution, where the trim algorithm has forced the dynamic inflow model to show an increase in angle of attack over the entire rotor disk to yield equivalence with the tip-loaded distribution predicted by the vorticity-transport model. Similar effects are noticeable too in the lateral and longitudinal gradients of the angle-of-attack distribution in the forward flight case.

Incorporation of a more comprehensive rotor-dynamic model, for instance one that allows excitation of the first torsional mode of the blade, will permit the rotor to respond to the higher-order moments of the loading distribution, and such an enhancement of the approach described here may indeed be necessary for the more detailed description of the blade loading inherent in the vorticity transport model to appear as a marked improvement in the prediction of the lateral dynamics. Note, though, that even within the confines of the present rotor–fuselage formalism, where it is to be expected that aerodynamic interactions are significant enough to affect even the low-order moments of the loading distribution on the rotor disk, such as in the case of the tail rotor, marked separation between the predictions of the two models is indeed observed. The tail rotor collective pitch predicted with the vorticity transport model, with its more realistic portrayal of the aerodynamic interaction between the main and tail rotors, is significantly closer to the flight data than the similar prediction made with the dynamic inflow model.

Taken together, these observations suggest that the level of fidelity of the rotor-dynamic model and of the wake model cannot be seen in isolation from each other as previously thought and, hence, that overall improvement in the fidelity of rotorcraft simulations may not follow the gradual evolution in complexity suggested by Padfield's hierarchical paradigm. Instead, a significant improvement in modeling fidelity may only be achieved by a single, integrated, jump in complexity of several simultaneous aspects of the flight dynamic model.

Conclusion

The results presented in this paper largely support the existing view that correct prediction of the aerodynamics associated with real flow features such as wake distortion, blade–vortex interactions, and main rotor/tail rotor interaction is an important contributing factor to the overall fidelity of rotorcraft flight-dynamic simulations. This conclusion is supported by the improvement in prediction, relative to flight data, of the important cross-coupling derivatives, airframe response to control inputs, vibration levels, and trim parameters made with an induced velocity model that reproduces these features, when compared against predictions made with a model from which these effects are absent. Furthermore, the results presented here suggest that although wake modeling fidelity is important in the capture of some of the subtleties of the trimmed state of the aircraft, comprehensive incorporation of real-wake effects may have even greater relevance as simulation bandwidth is increased. Finally, analysis of discrepancies in the prediction of trim states made with the two induced velocity models supports the argument that simulation fidelity cannot be isolated into separate issues of wake fidelity and rotor-dynamic fidelity and strongly suggests that any significant increase in overall fidelity of rotorcraft simulations will not be attained by our following a simple hierarchical progression of model complexity.

Acknowledgments

The research leading to this paper was conducted under the ongoing Engineering and Physical Sciences Research Council Grant GR/L 19614. The authors wish to acknowledge the valuable contribution of A. T. McCallum of the Defence Evaluation and Research Agency, Bedford, England, United Kingdom.

References

[1]Padfield, G. D., "Theoretical Modelling for Helicopter Flight Dynamics: Development and Validation," International Council for the Aeronautical Sciences, ICAS-88-6.1.3, Jerusalem, Israel, 1988, pp. 165–177.

[2]Theodore, C., and Celi, R., "Flight Dynamic Simulation of Hingeless Rotor Helicopters Including a Maneuvering Free Wake Model," *Proceedings of the American Helicopter Society 54th Annual Forum*, American Helicopter Society, Alexandria, VA, 1998.

[3]Gaonkar, G. H., and Peters, D. A., "A Review of Dynamic Inflow Modeling for Rotorcraft Flight Dynamics," *Vertica*, Vol. 12, No. 3, 1988, pp. 213–242.

[4]Peters, D. A., and HaQuang, N., "Dynamic Inflow for Practical Applications," *Journal of the American Helicopter Society*, Vol. 33, No. 4, 1988, pp. 64–68.

[5]Chen, R. T. N., "A Survey of Nonuniform Inflow Models for Rotorcraft Flight Dynamics and Control Applications," *Vertica*, Vol. 14, No. 2, 1990, pp. 147–184.

[6]Krothapalli, K. R., Prasad, J. V. R., and Peters, D. A., "A Generalized Dynamic Wake Model with Wake Distortion Effects," *Proceedings of the American Helicopter Society 54th Annual Forum*, American Helicopter Society, Alexandria, VA, 1998, pp. 527–535.

[7]Rosen, A., Yaffe, R., Mansur, M. H., and Tischler, M. B., "Methods for Improving the Modeling of Rotor Aerodynamics for Flight Mechanics Purposes," *Proceedings of the American Helicopter Society 54th Annual Forum*, American Helicopter Society, Alexandria, VA, 1998, pp. 1337–1355.

[8]Houston, S. S., and Tarttelin, P. C., "Validation of Mathematical Simulations of Helicopter Vertical Response Characteristics in Hover," *Journal of the American Helicopter Society*, Vol. 36, No. 1, 1991, pp. 45–57.

[9]Padfield, G. D., and DuVal, R. W., "Application Areas for Rotorcraft System Identification Simulation Model Validation," LS178, AGARD, 1991, pp. 12.1–12.39.

[10]Houston, S. S., "Rotorcraft Aeromechanics Simulation for Control Analysis: Mathematical Model Definition," Rept. 9123, Dept. of Aerospace Engineering, Univ. of Glasgow, Glasgow, Scotland, U.K., 1991.

[11]Turnour, S. R., and Celi, R., "Modelling of Flexible Rotor Blades for Helicopter Flight Dynamics Applications," *Journal of the American Helicopter Society*, Vol. 41, No. 1, 1996, pp. 52–61.

[12]Peters, D. A., and He, C. J., "Finite State Induced Flow Models, Part II: Three-Dimensional Rotor Disk," *Journal of Aircraft*, Vol. 32, No. 2, 1995, pp. 323–333.

[13]Brown, R. E., "Rotor Wake Modeling for Flight Dynamic Simulation of Helicopters," *AIAA Journal*, Vol. 38, No. 1, 2000, pp. 57–63.

[14]Houston, S. S., "Validation of a Non-Linear Individual Blade Rotorcraft Flight Dynamics Model Using a Perturbation Method," *Aeronautical Journal*, Vol. 98, No. 977, 1994, pp. 260–266.

[15]Houston, S. S., "Validation of a Blade-Element Helicopter Model for Large-Amplitude Manoeuvres," *Aeronautical Journal*, Vol. 101, No. 1001, 1997, pp. 1–7.

[16]Houston, S. S., "Validation of a Rotorcraft Mathematical Model for Autogyro Simulation," *Journal of Aircraft* (submitted for publication).

[17]Bramwell, A. R. S., *Helicopter Dynamics*, Arnold, London, 1976, pp. 1–13.

[18]Schumann, U., and Sweet, R. A., "A Direct Method for the Solution of Poisson's Equation with Neumann Boundary Conditions on a Staggered Grid of Arbitrary Size," *Journal of Computational Physics*, Vol. 20, No. 2, 1976, pp. 171–182.

[19]Toro, E. F., "A Weighted Average Flux Method for Hyperbolic Conservation Laws," *Proceedings of the Royal Society of London, Series A: Mathematical and Physical Sciences*, Vol. 423, No. 1864, 1989, pp. 401–418.

[20]Padfield, G. D., "SA 330 Puma Identification Results," LS178, AGARD, 1991, pp. 10.1–10.38.